Supporting Information

for

Recreation of ultrasoundand temperature-triggered bubble liposome from economic precursors to enhance the therapeutic efficacy of curcumin in cancer cells

Santanu Patra,[a] Ekta Roy,[a] Rashmi Madhuri,[a,*] Prashant K. Sharma[b]

[a]Department of Applied Chemistry, Indian School of Mines, Dhanbad, Jharkhand 826 004, INDIA

[b]Functional Nanomaterials Research Laboratory, Department of Applied Physics, Indian School of Mines, Dhanbad, Jharkhand 826 004, INDIA

*Corresponding Author. Tel: +91 9471191640. Email: rshmmadhuri@gmail.com (R. Madhuri)

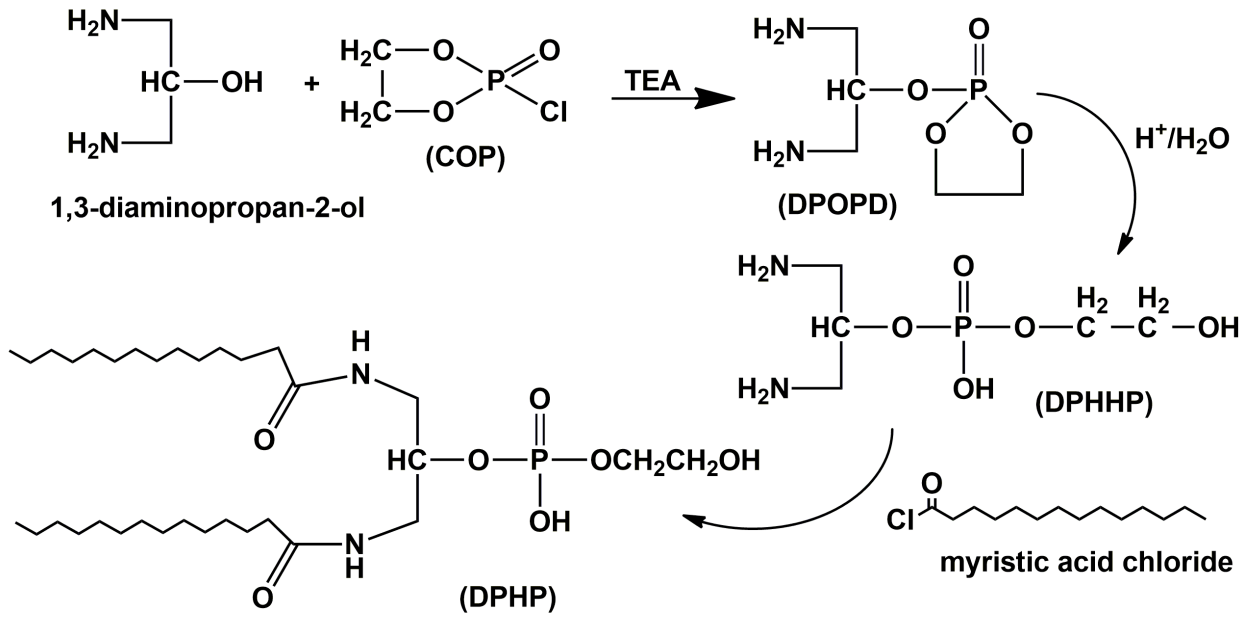

COP: 2-chloro-1,3,2-dioxaphospholane 2-oxide
DPOPD: 2-((1,3-diaminopropan-2-yl)oxy)-1,3,2-dioxaphospholane 2-oxide
DPHHP: 1,3-diaminopropan-2-yl (2-hydroxyethyl) hydrogen phosphate
DPHP: 1,3-ditetradecanamidopropan-2-yl (2-hydroxyethyl) hydrogen phosphate

Scheme S1: Schematic diagram showing the preparational procedure of DPHP.

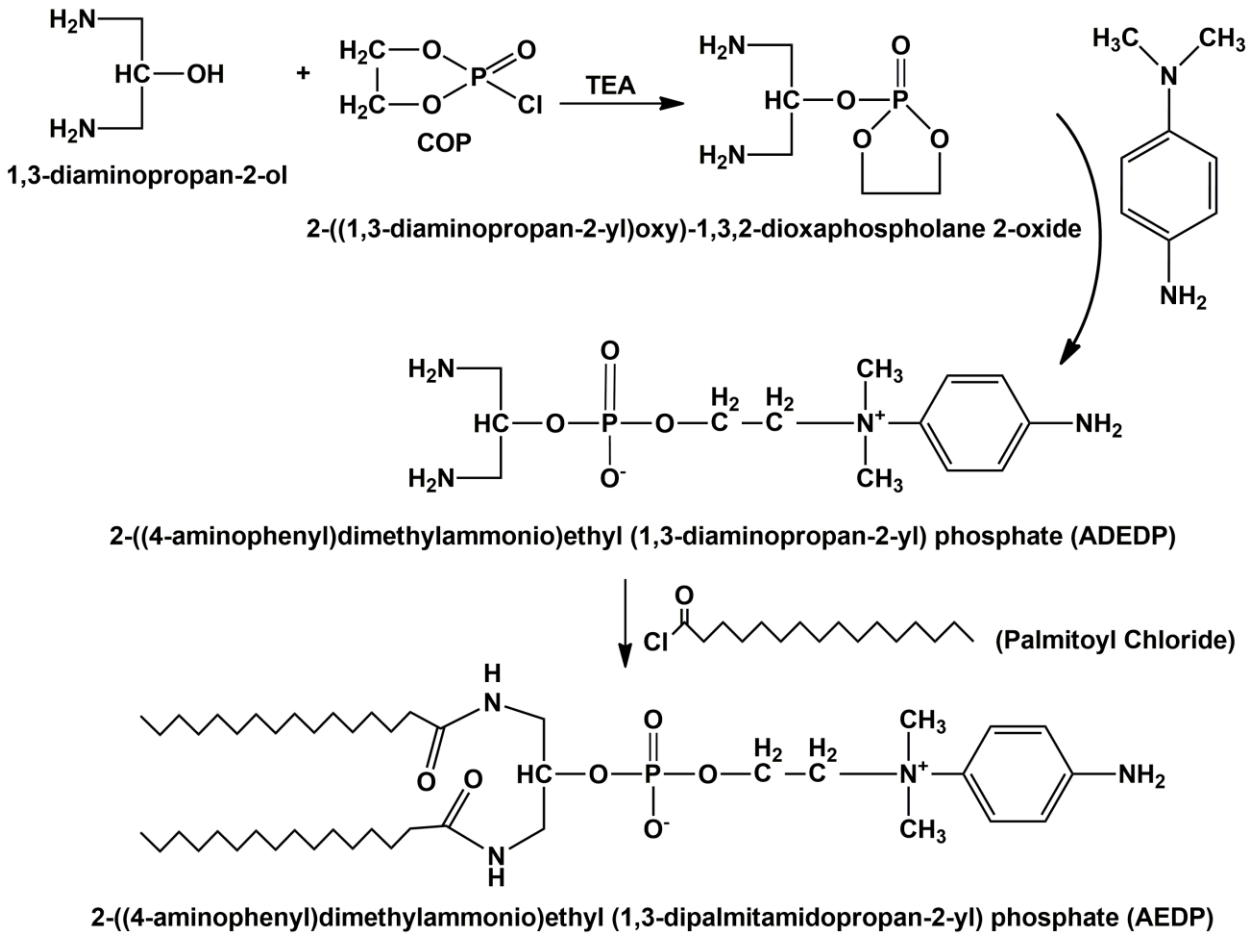

Scheme S2: Schematic diagram showing the preparational procedure of AEDP.

S1. Preparation of palmitoyl and myristoyl chloride

Palmitoyl and myristoyl chloride was prepared by a simple procedure using thionyl chloride. In brief, palmitic acid/myristic acid (0.1 mol) dissolved in 25 mL THF and to it thionyl chloride (0.1 mol) was added drop wise. The reaction mixture was then condensed for six hours. The product obtained after evaporation was re-precipitated in dry THF.

S2. Chracterization of liposomic precursors by FT-IR and NMR

S2.1 1,3-ditetradecanamidopropan-2-yl (2-hydroxyethyl) hydrogen phosphite (DPHP)

A three step method was used for the preparation of DPHP. In the first step, COP and 1,3-diamino-2-propanol reacted to give 2-((1,3,2-dioxaphospholan-2-yl)oxy)propane-1,3-diamine (DPOPD). The second step is the hydrolysis by acetic acid to give 1,3-diaminopropan-2-yl (2-hydroxyethyl) hydrogen phosphate (DPHHP). In the last step hydrophobic chain was attached by reaction with palmitoyl chloride to five DPHP.

The preparation of DPOPD can be characterized by FT-IR spectroscopic study. As can be seen, in the FT-IR spectra of DPOPD (Figure S1), the presence characteristics peak for N-H stretch (3150 cm^{-1}), N-H bend (1580 cm^{-1}), P=O stretch (1400 cm^{-1}), C-O stretch (1250 cm^{-1}) and C-N stretch (1100 cm^{-1}) confirms the formation DPOPD. After the hydrolysis, in the FT-IR spectra of DPHHP (Figure S2) an additional broad peak at 3550 cm^{-1} appears (due to O-H stretch). All others peak remains in the similar position as that of DPOPD. This proves the successful hydrolysis of product. In the last step, after the reaction with myristoyl chloride, along with all the characteristics peak of DPHHP, an extra peak at 1700 cm^{-1} due to the C=O stretch can be observed (Figure S3). This may be due to the formation of amide linkage after the binding with myristoyl chloride.

The formation of final product (DPHP) is further characterized by ^{1}H-NMR spectroscopy. The ^{1}H-NMR spectra is represented in Figure S4 and were in accordance with the proposed structure of the product. The blue color numerical values represents the corresponding chemical shift values of each proton. The proves the successful formation of DPHP.

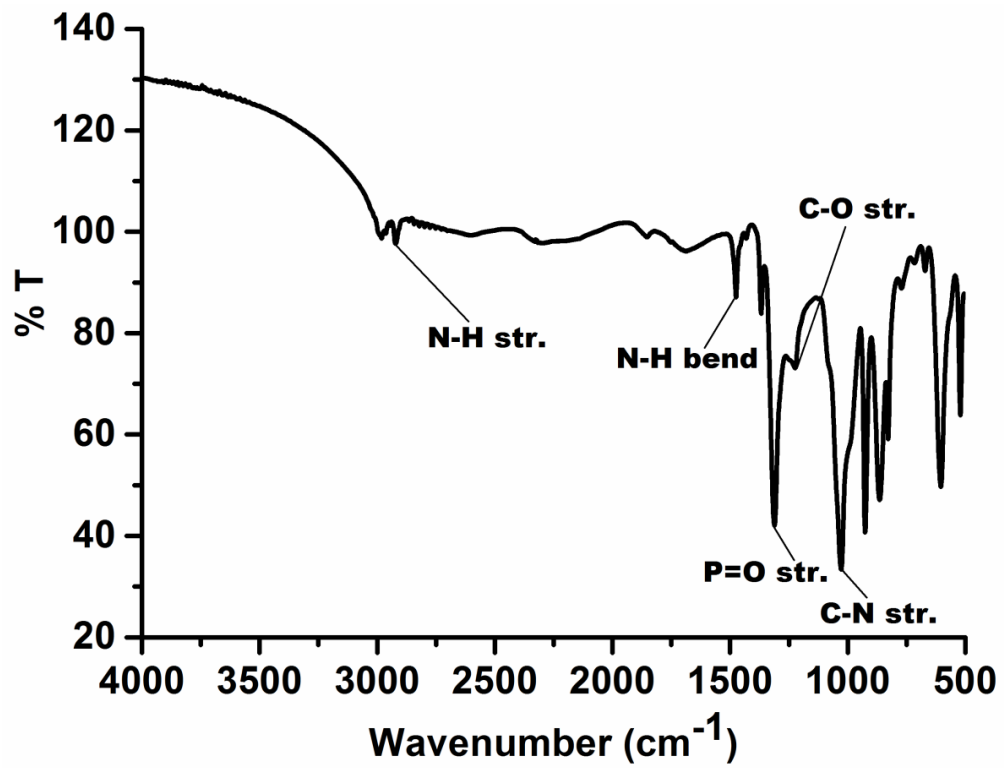

Figure S1: FT-IR spectra of 2-((1,3,2-dioxaphospholan-2-yl)oxy)propane-1,3-diamine, DPOPD.

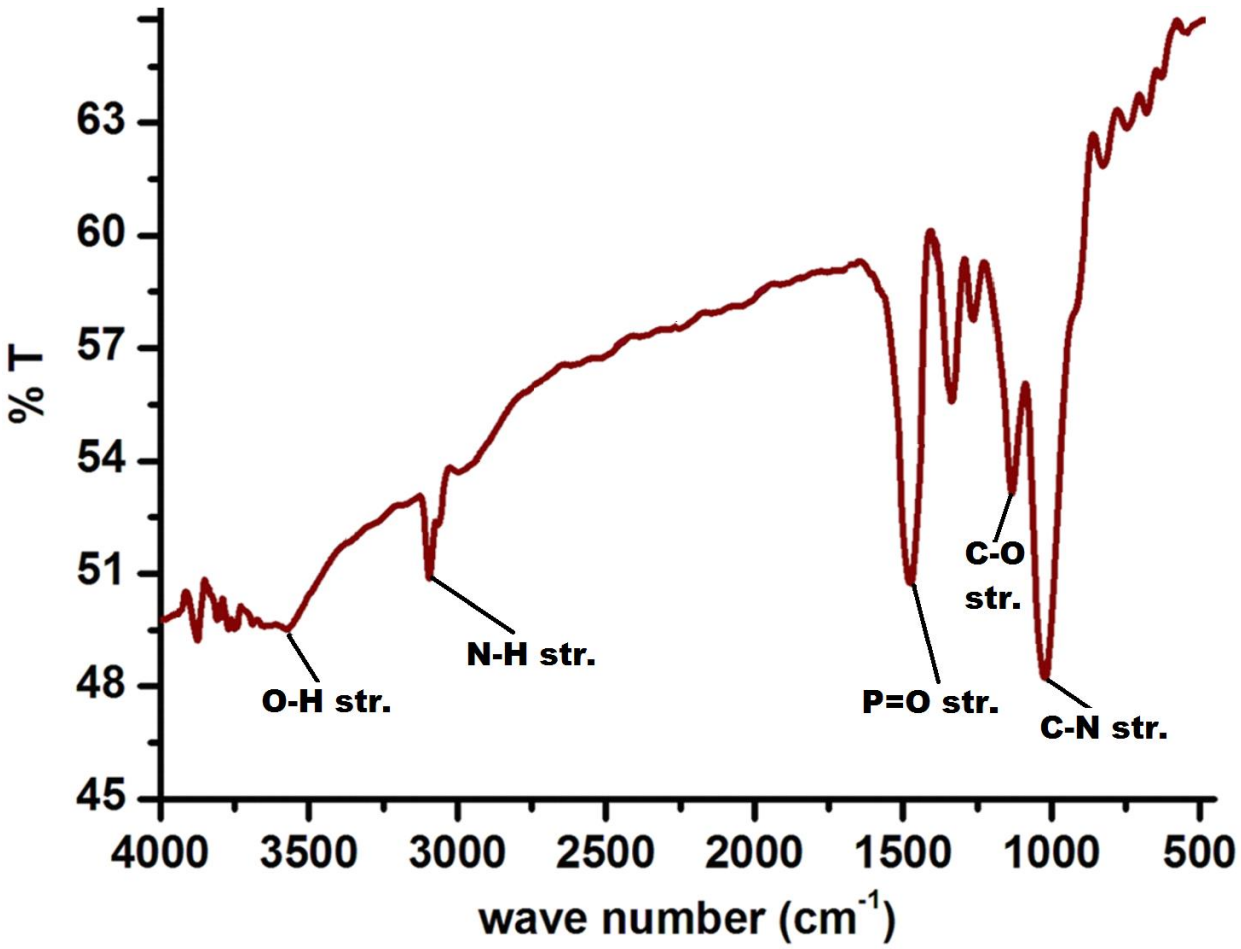

Figure S2: FT-IR spectra of 1,3-diaminopropan-2-yl (2-hydroxyethyl) hydrogen phosphate, DAHHP.

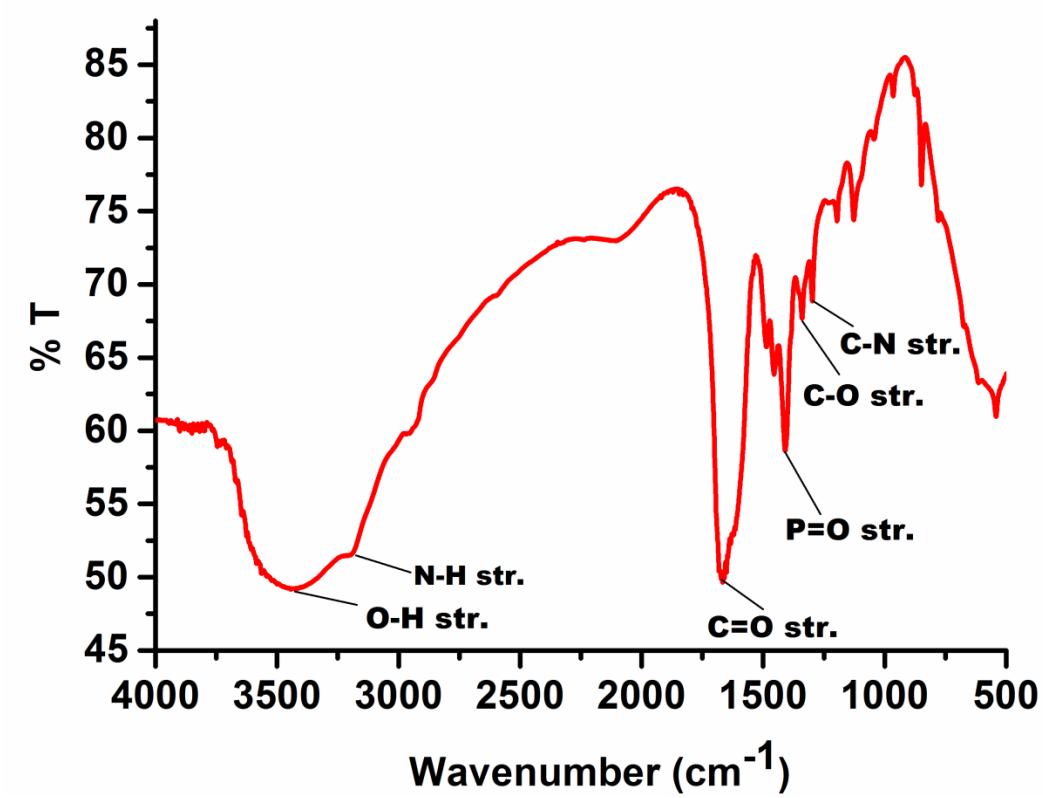

Figure S3: FT-IR spectra of 1,3-ditetradecanamidopropan-2-yl (2-hydroxyethyl) hydrogen phosphite, DPHP.

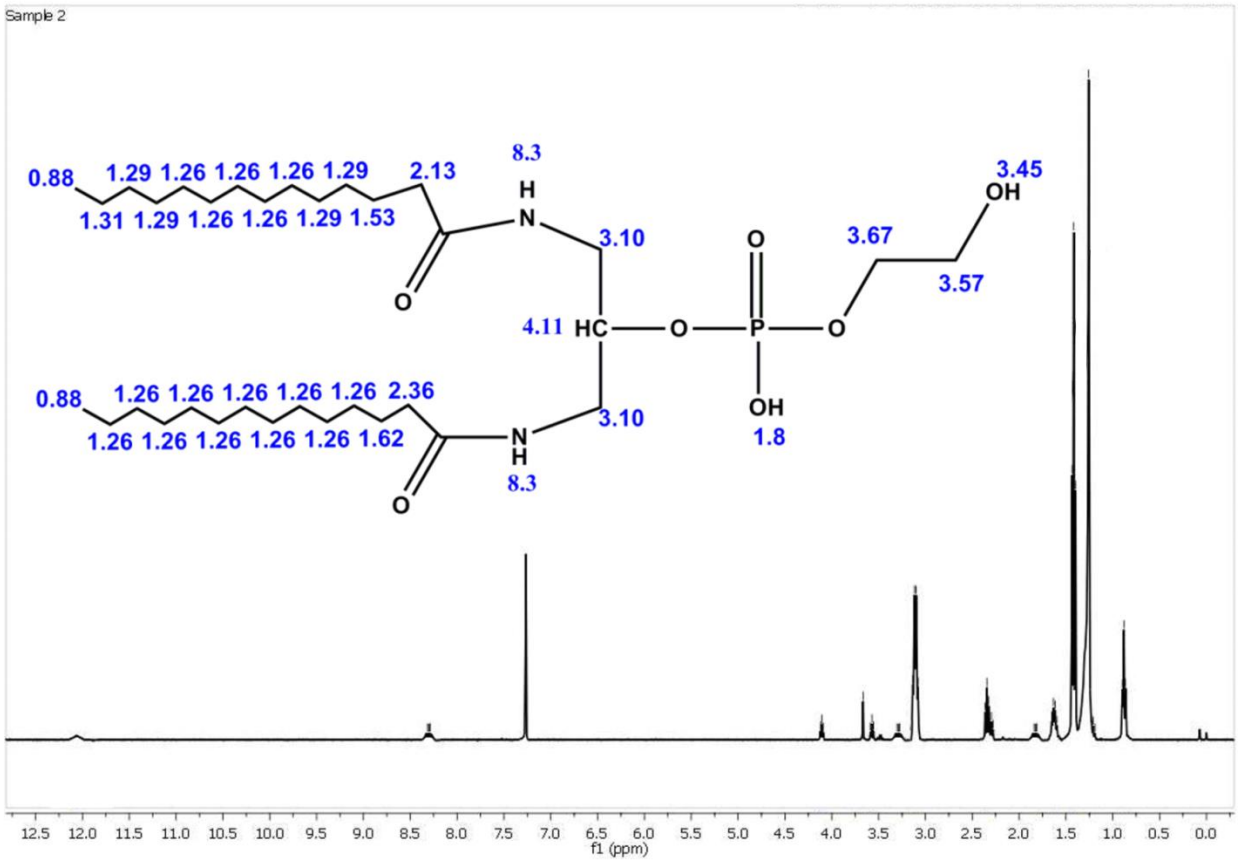

Figure S4: NMR spectra of 1,3-ditetradecanamidopropan-2-yl (2-hydroxyethyl) hydrogen phosphite (DPHP).

S2.2. 2-((4-aminophenyl)dimethylammmonio)ethyl (1,3-dipalmitamidopropan-2-yl)phosphite (AEDP)

Like DPHP, AEPD was also prepared by three steps method. First step was the preparation of DPOPD, characterization discussed in the preveous section. The second step is ring opening by N,N-dimethyl paraphenylene diamine to give 2-((4-aminophenyl)dimethylammonio)ethyl (1,3-diaminopropan-2-yl) phosphite (AEDPP) and the last step was palmitoyl group modification to give AEDP.

AEDPP was characterized by FT-IR spectroscopy. In the FT-IR spectra of AEDPP (Figure S5), all the characteristics peak of its precursor DPOPD was present as for N-H stretch (3150 cm^{-1}), N-H bend (1580 cm^{-1}), P=O stretch (1400 cm^{-1}), C-O stretch (1250 cm^{-1}) and C-N stretch (1100 cm^{-1}) along with an extra peak at 1680 cm^{-1} for C=C stretch (due to the

modification of aromatic diamine). Looking into the FT-IR spectra of AEDP (Figure S6), an additional C=O stretch (1680 cm^{-1}) obtained due the bonding with palmitioyl chloride.

AEDP was also characterized by ^{1}H-NMR spectroscopy and plotted in Figure S7. All the hydrogen with their corresponding chemical shift can be assigned and portrayed in blue color. This as prepared AEDP was used for the preparation of liposome.

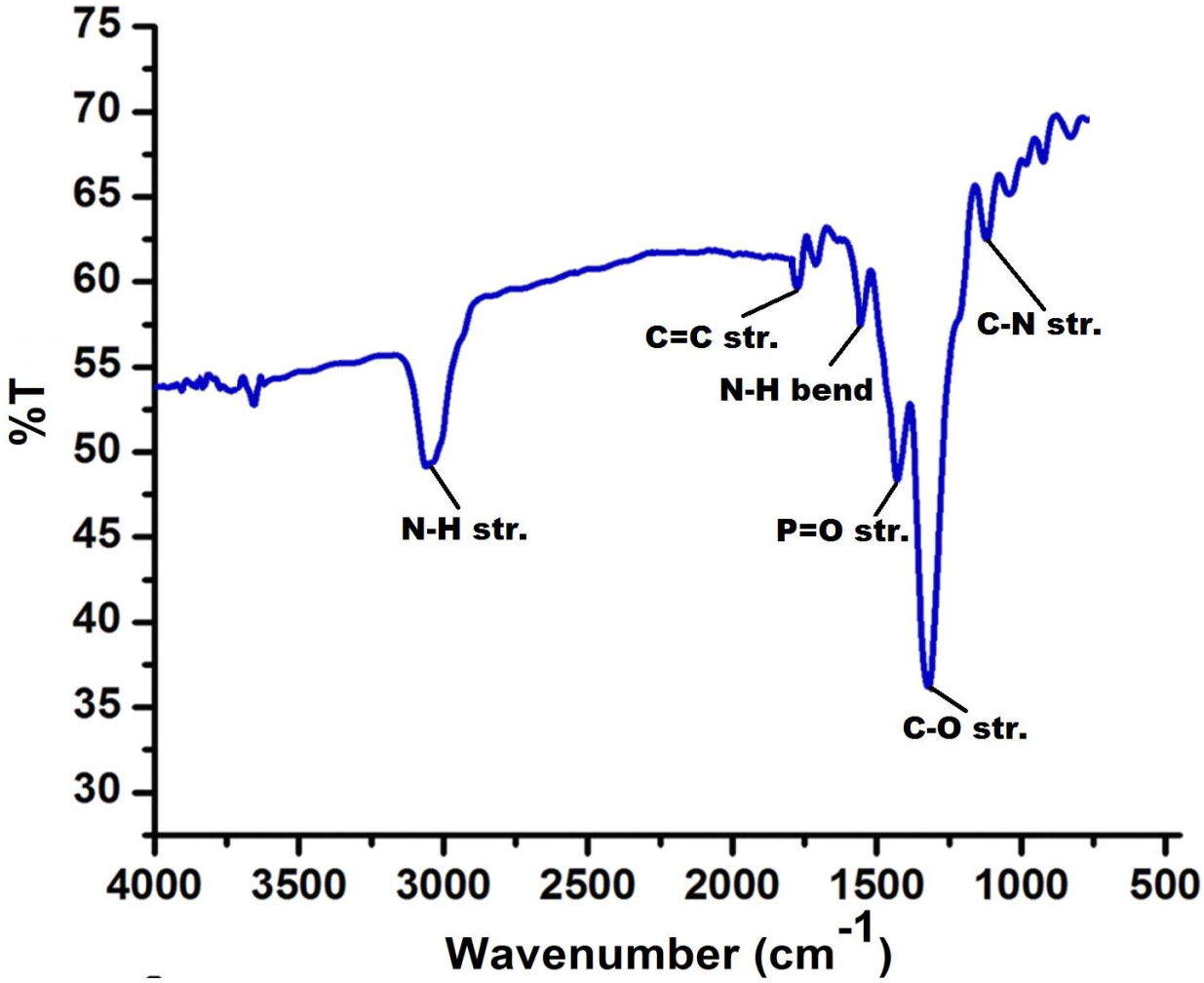

Figure S5: FT-IR spectra of 2-((4-aminophenyl)dimethylammonio)ethyl (1,3-diaminopropan-2-yl) phosphite (AEDPP).

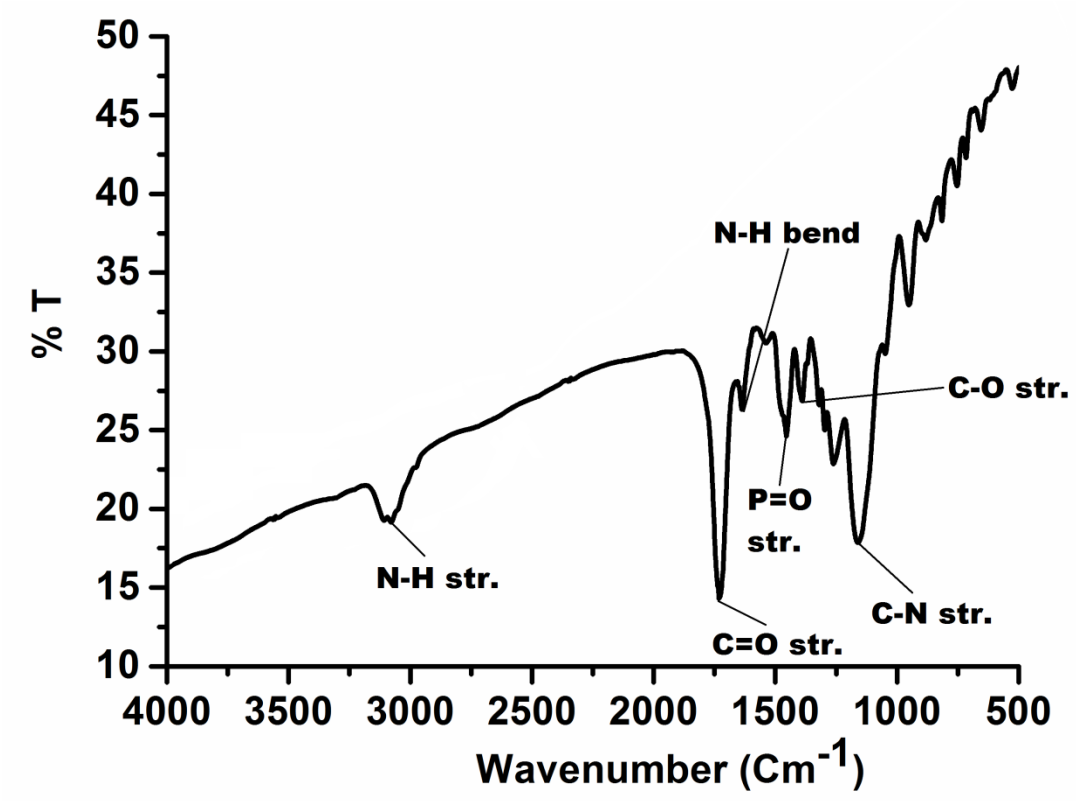

Figure S6: FT-IR spectra of 2-((4-aminophenyl)dimethylammmonio)ethyl (1,3-dipalmitamidopropan-2-yl)phosphite (AEDP).

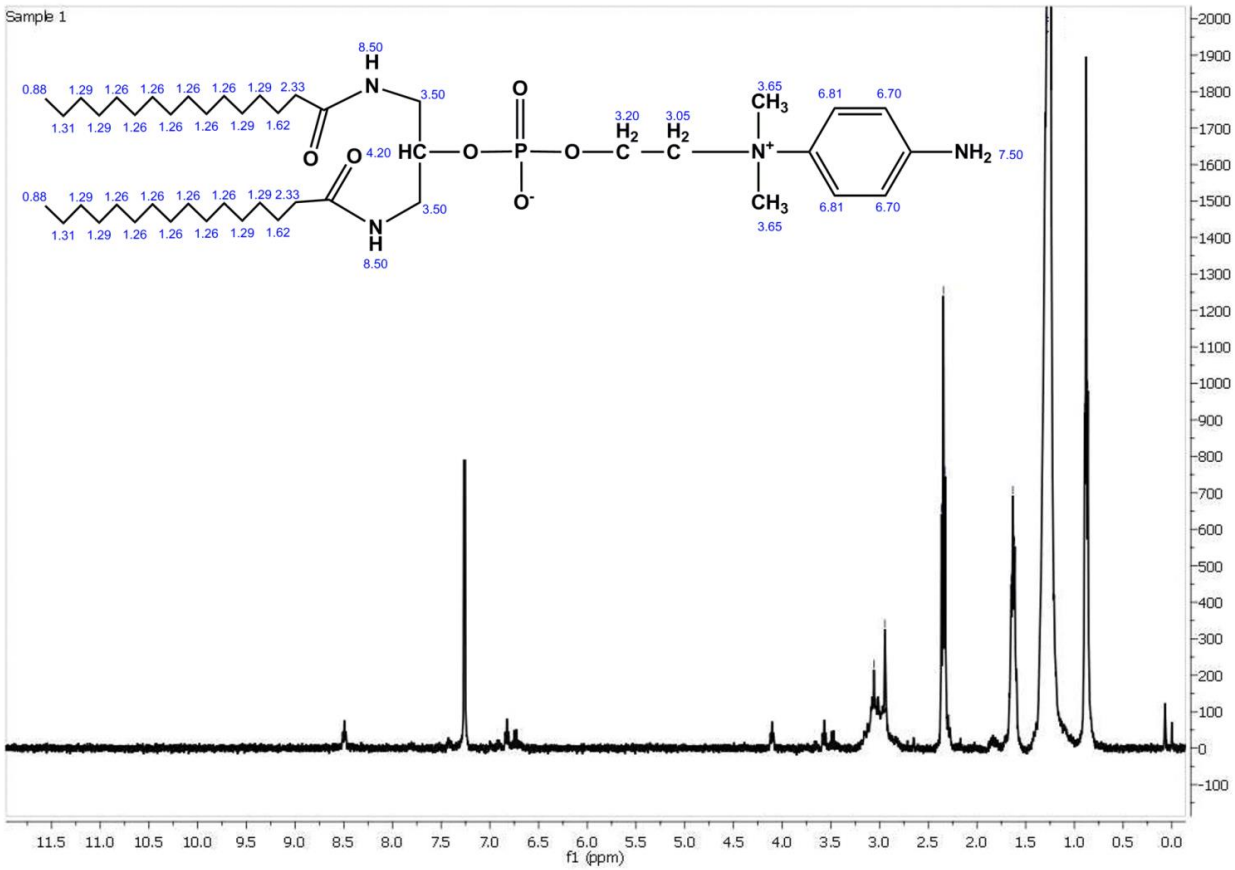

Figure S7: NMR spectra of 2-((4-aminophenyl)dimethylammmonio)ethyl (1,3-dipalmitamidopropan-2-yl)phosphite (AEDP).

S2.3. Folic acid-Cholesterol conjugate (FA-Ch)

FA-Ch was characterized by means of F-IR spectra and ^{1}H-NMR spectra. Looking into the FT-IR spectra of FA-Ch (Figure S8), the characteristics peak for folic and cholesterol can be seen (3100 cm^{-1}, N-H stretch; 2800 cm^{-1}, C-H stretch; 1580 cm^{-1}, N-H bend; 1240 cm^{-1}, C-O stretch; 1120 cm^{-1}, C-N stretch and 1000 cm^{-1}, C-O-C stretch) along with an extra peak at 1670 cm^{-1} due to the bonding between this two. In the 1H-NMR spectra (Figure S9), it can be clearly visualized that all the hydrogen with chemical shift values are in accordance with their structure.

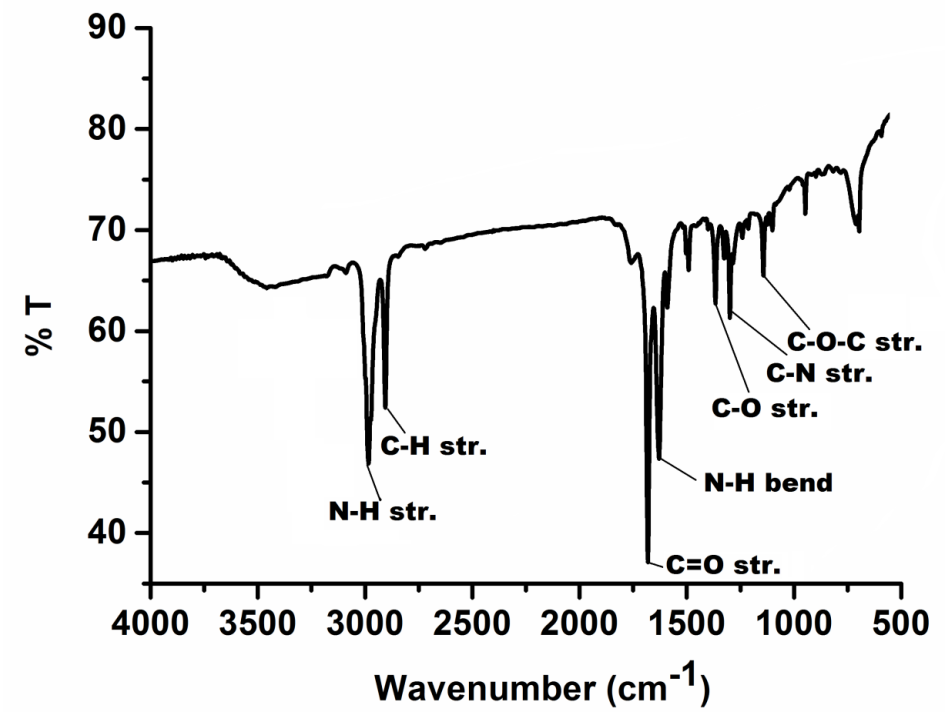

Figure S8: FT-IR spectra of folic acid-Cholesterol conjugates (FA-Ch).

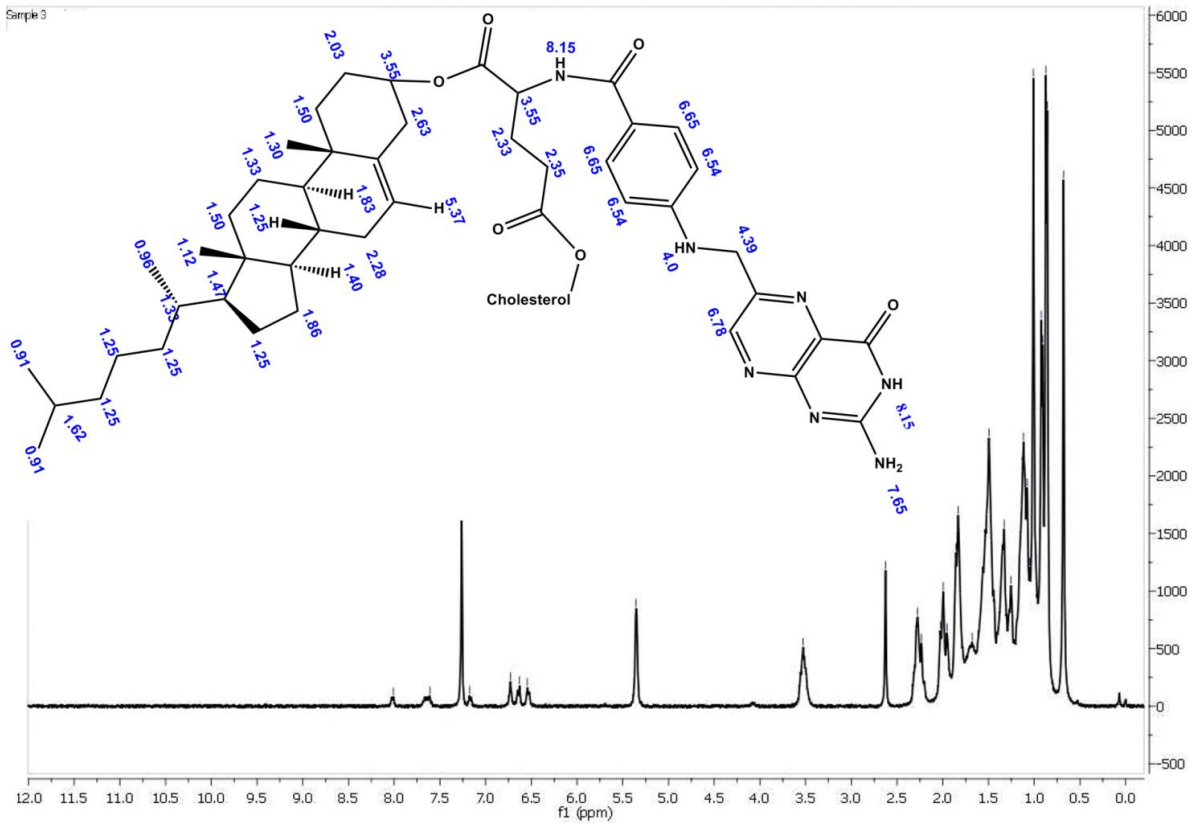

Figure S9: NMR spectra of folic acid-cholesterol conjugate (FA-Ch).

S2.4. Fluorescein dye-Cholesterol conjugates (FL-Ch)

In the FT-IR spectra (Figure S10) fluorescein dye-cholesterol conjugate (FL-Ch), characteristics peaks for both fluorescein dye and cholesterol can be observed (3100 cm^{-1}, N-H stretch; 2800 cm^{-1}, C-H stretch; 1580 cm^{-1}, N-H bend; 1240 cm^{-1}, C-O stretch; 1120 cm^{-1}, C-N stretch and 1000 cm^{-1}, C-O-C stretch). The extra peak at 1690 cm^{-1} can be assigned to the C=O stretch due to binding between them. The 1H-NMR spectra is also in accordance with the structure as can be seen in the Figure S11.

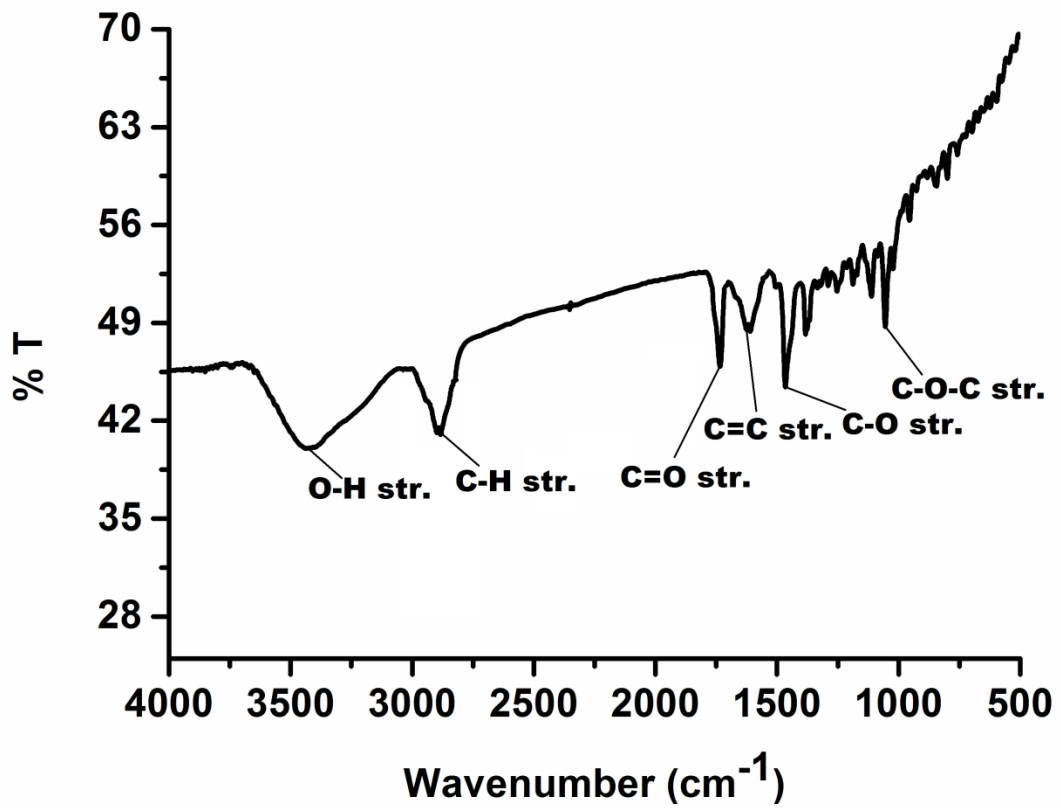

Figure S10: FT-IR spectra of fluorescein dye-cholesterol conjugates (FL-Ch).

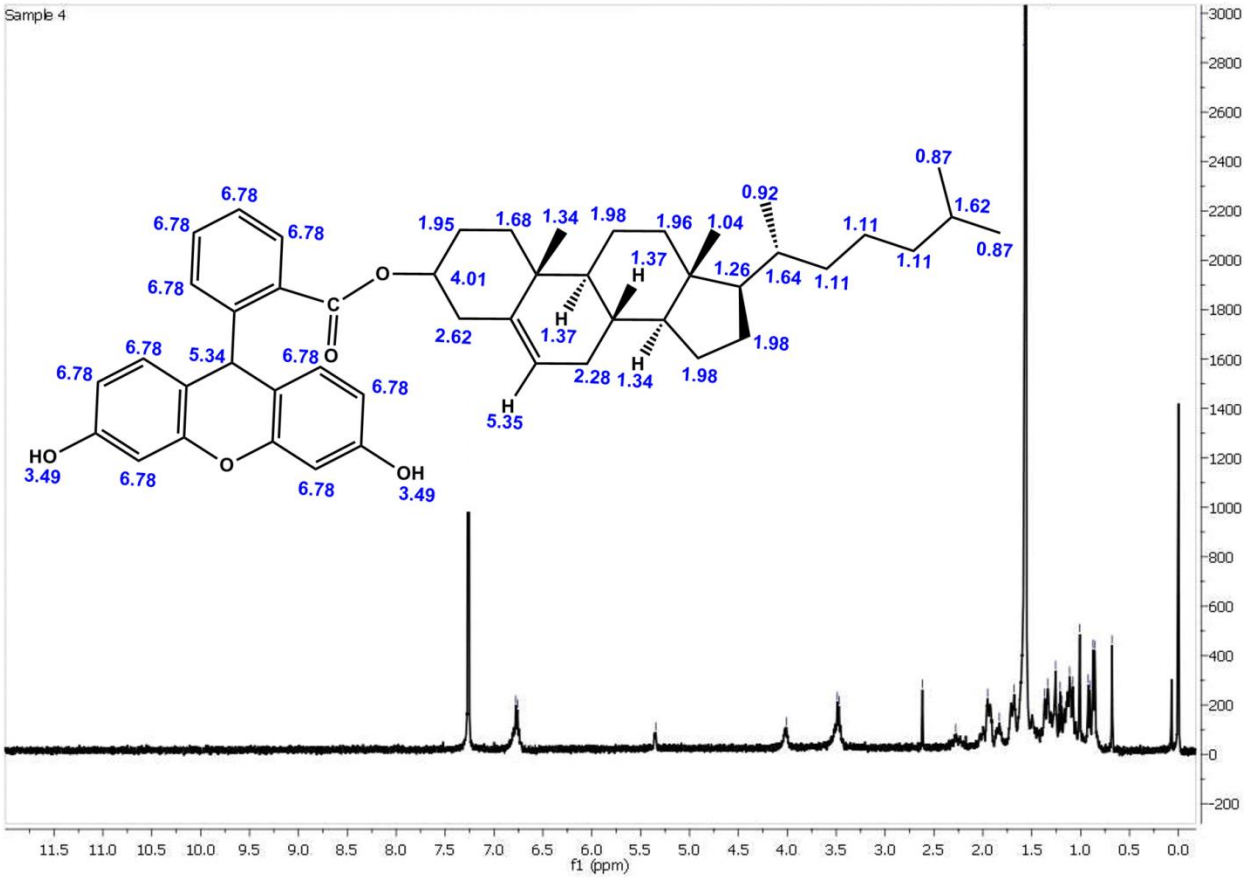

Figure S11: NMR spectra of fluorescein dye-cholesterol conjugate (FL-Ch).

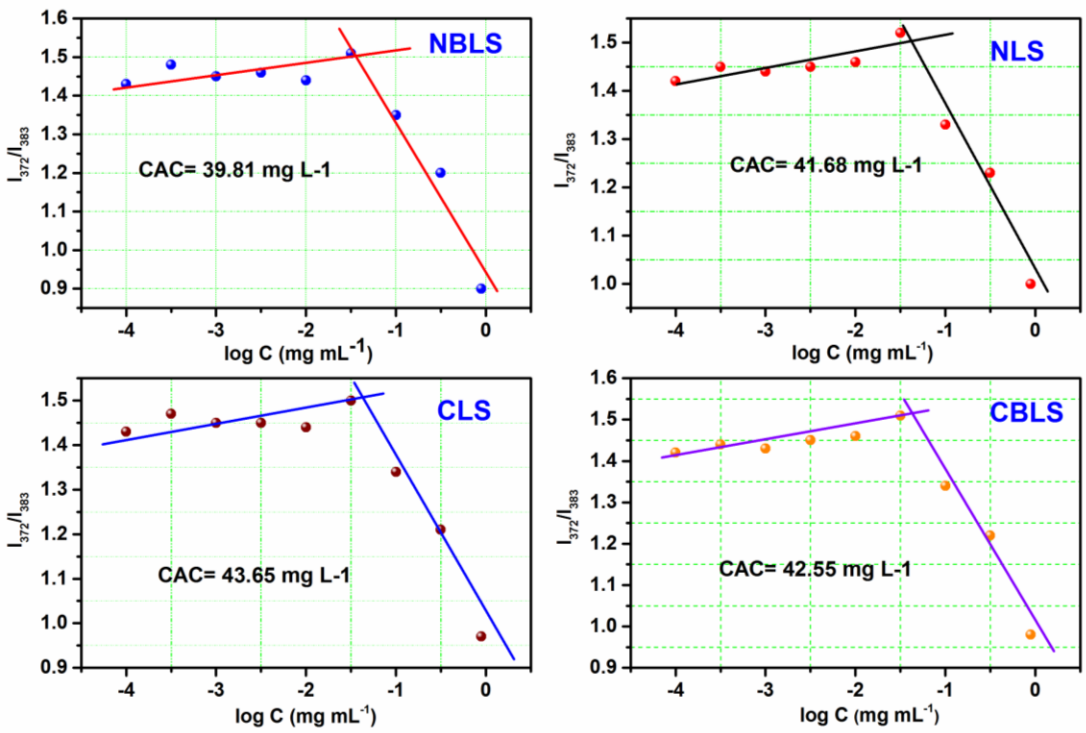

Figure S12 : Determination of CAC value of NBLS, NLS, CLS and CBLS.

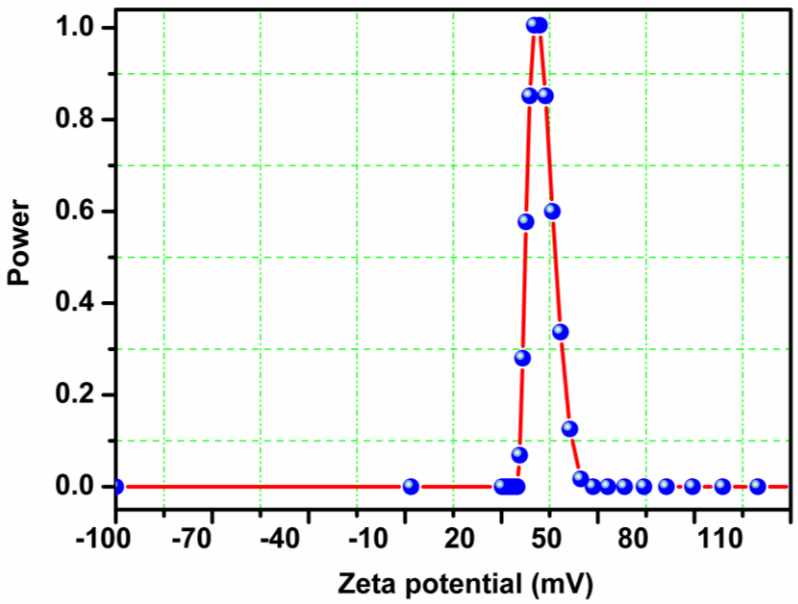

Figure S13: Zeta potential plot for NBLS.

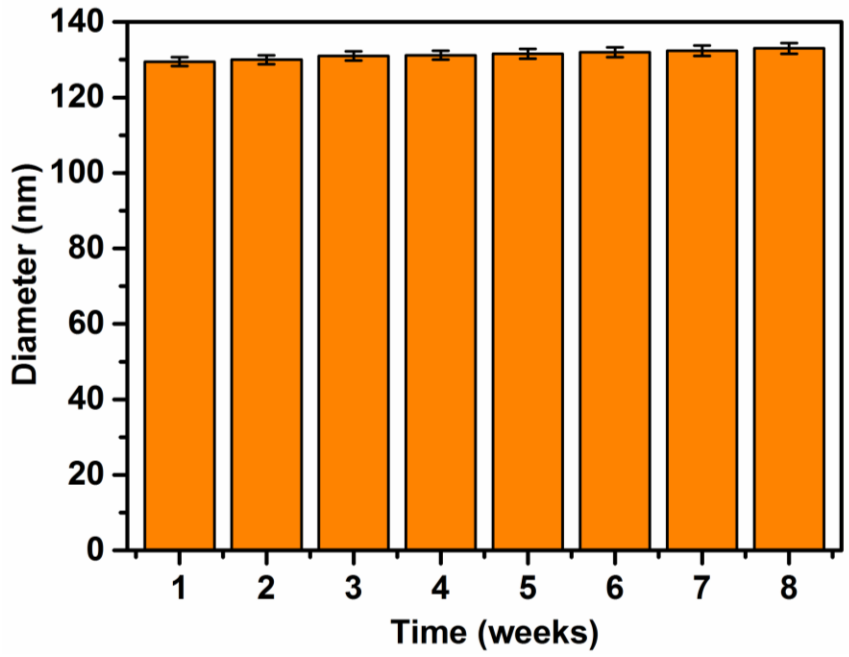

Figure S14: Change in hydrodynamic diameter upon storage at room tempeterature.

Table S1: Comparison with other nanocarriers reported in literature for curcumin delivery.

S.N.	Materials used	Particle size (nm)	% EE	Release time	% Release	Reference
1.	Bubble liposome	150.5	96.2	1 min	60	S1
2.	Poly-SPIONs	37	98	150 min	85	S2
3.	SLN	152.8	90	72 h	70	S3
4.	Transferrin mediated SLN	194	77.27	48 h	84.3	S4
5.	CS/PCL NPs	220-360	70.9	5 days	68	S5
6.	CUR-MSNs	217-234	-	180 min	~75	S6
7.	mPEG-zein polymeric micelle	95-125	95	24 h	~80	S7
8.	Liposome-PEG-PEI complex	258-269	45	120 h	90	S8
9.	Bubble liposome	129.5	96.7	2 min	90	This work

EE= encapsulation efficiency, SLN = Solid Lipid Nanoparticles, CS/PCL= chitosan/poly(Ɛ-caprolactone), CUR-MSNs = Curcumin-mesoporous silica nanoparticles, mPEG-zein = Methoxy poly(ethylene glycol)-zein, PEG-PEI= Polyethylene glycol-polyethylenimine.

Reference:

S1. K. -J. Chen, E. -Y. Chaung, S. -P. Wey, K. -J. Lin, F. Cheng, C. -C. Lin, H. - L. Liu, H. -W. Tseng, C. -P. Liu, M. -C. Wei; C. -M. Liu and H. -W. Sung, Hyperthermia mediated local drug delivery by a bubble-generating liposomal system for tumor-specific chemotherapy, *ACS Nano*, 2014, **8**, 5105-5115.

S2. S. Patra, E. Roy, P. Karfa, S. Kumar, R. Madhuri and P. K. Sharma, Dual-Responsive Polymer Coated Superparamagnetic Nanoparticle for Targeted Drug Delivery and Hyperthermia Treatment*ACS Appl. Mater. Interfaces*, 2015, **7**, 9235-9246.

S3. J. Sun, C. Bi, H. M. Chan, S. Sun, Q. Zhang and Y. Zheng, Curcumin-loaded solid lipid nanoparticles have *in vitro* antitumour activity, cellular uptake, and improved *in vivo* bioavailability, *Colloid Surf., B*, 2013, **111**, 367-375.

S4. R. S. Mulik, J. Mönkkönen, R. O. Juvonen, K. R. Mahadik and A. R. Paradkar, Transferrin mediated solid lipid nanoparticles containing curcumin: enhanced *in vitro* anticancer activity by induction of apoptosis, *Int. J. Pharm.*, 2010, **398**, 190-203.

S5. J. Liu, L. Xu, C. Liu, D. Zhang, S. Wang, Z. Deng, W. Lou, H. Xu, Q. Bai and J. Ma, Preparation and characterization of cationic curcumin nanoparticles for improvement of cellular uptake, *Carbohydr. Polym.*, 2012, **90**, 16-22.

S6. S. Kim, S. Philippot, S. Fontanay, R. E. Duval, E. Lamouroux, N. Canilho and Andreea Pasc, pH and glutathione responsive release of curcumin from mesoporous silica nanoparticles coated using tannic acid-Fe (III) complex, *RSC Adv.*, 2015, **5**, 90550-90558.

S7. S. Podaralla, R. Averineni, M. Alqahtani and O. Perumal, Synthesis of novel biodegradable methoxy poly(ethylene glycol)-Zein micelles for effective delivery of curcumin, *Mol. Pharmaceutics*, 2012, **9**, 2778−2786.

S8. Y. -L. Lin, Y. -K. Liu, N. -M. Tsai, J. -H. Hsieh, C. -H. Chen, C. -M. Lin and K. -W. Liao, A Lipo-PEG-PEI complex for encapsulating curcumin that enhances its antitumor effects on curcumin-sensitive and curcumin-resistance cells, *Nanomedicine*, 2012, **8**, 318-327.